

Original article

## Assimilation of Ice Concentration Data through a Strongly Coupled Regime in the Arctic Ocean Model

M. N. Kaurkin<sup>1, ✉</sup>, L. Yu. Kalnitskii<sup>1</sup>, K. V. Ushakov<sup>1</sup>, R. A. Ibrayev<sup>1, 2</sup>

<sup>1</sup> Shirshov Institute of Oceanology, Russian Academy of Sciences, Moscow, Russian Federation

<sup>2</sup> Marchuk Institute of Numerical Mathematics, Russian Academy of Sciences, Moscow, Russian Federation

✉ kaurkin.mn@ocean.ru

### Abstract

**Purpose.** The purpose of this study is to develop and implement a strongly coupled approach to the assimilation of available observational data in a coupled ocean-sea ice circulation model, and to test it for the Arctic region.

**Methods and Results.** In the coupled INMIO (ocean) and CICE 5.1 (ice) model at 0.25° resolution, the data were assimilated using the Compact Modeling Framework (CMF3.0) platform with the DAS (Data Assimilation Service) software based on the EnOI (Ensemble Optimal Interpolation) method. A strongly coupled assimilation approach was applied. This approach involves simultaneous adjustment of the fields of water temperature, salinity, sea level, and ice concentration using observational data (ARGO profiles, AVISO satellite altimetry, and OSI SAF ice concentration). A specialized interface was developed to redistribute the integrated ice concentration among the ice thickness categories. Numerical experiments with and without data assimilation were performed for 2020. It is shown that data assimilation through a strongly coupled regime reduces the average error in reproducing the ice area from 27 to 7% as compared to the NSIDC data. The standard error of ocean surface water temperature is reduced to 1.0 °C, and that of ice concentration in the edge area to 0.2. The model fields correspond better to the independent OSTIA data.

**Conclusions.** The developed approach to the strongly coupled assimilation of oceanic and ice data in the coupled ocean-ice model provides a significant increase in the accuracy of forecasting the condition both of the water and the ice field in the Arctic Ocean. The software can be adapted to other models.

**Keywords:** computer modeling, numerical modeling, data assimilation, ocean dynamics model, ocean-ice model, parallel computing, Arctic region, sea ice cover

**Acknowledgments:** The study was carried out at the Shirshov Institute of Oceanology, Russian Academy of Sciences, with financial support of the Russian Science Foundation (grant No. 25-27-00400).

**For citation:** Kaurkin, M.N., Kalnitskii, L.Yu., Ushakov, K.V. and Ibrayev, R.A., 2025. Assimilation of Ice Concentration Data through a Strongly Coupled Regime in the Arctic Ocean Model. *Physical Oceanography*, 33(2), pp. 352-365.

© 2026, M. N. Kaurkin, L. Yu. Kalnitskii, K. V. Ushakov, R. A. Ibrayev

© 2026, Physical Oceanography



## 1. Introduction

The Arctic Ocean (AO) plays an important role in the global climate system, where sea ice regulates the exchange of heat, moisture, and momentum between the atmosphere and the ocean. Arctic warming and changes in the hydrological cycle observed in recent decades have been accompanied by a wide range of processes in the ice-ocean system (see the review [1]).

Interpretation of such changes is extremely difficult due to the limited availability of observational data. Numerical modeling can significantly help in understanding these processes, but the lack of knowledge about the physics of ice-ocean interaction limits our ability to reproduce them realistically. An effective way to address this issue is to correct the dynamic model solution by assimilating observational data available at appropriate time scales.

The practice of numerical weather prediction has shown that coupled ocean-atmosphere models usually provide significantly more accurate forecasts than models of either medium alone. This has stimulated research into data assimilation approaches for coupled models that can significantly improve forecast quality [2]. A review of current activities in the field of coupled forecasting systems and data assimilation within these systems can be found in [3]. The materials of the World Meteorological Organization (WMO) Meeting on Coupled Data Assimilation define the differences between the approaches of *weakly and strongly coupled data assimilation* in atmosphere-ocean meteorological models [4]. In the weakly coupled approach, each component of the coupled system is corrected separately. In the strongly coupled approach, all variables and components of the coupled system are processed simultaneously in a single analysis.

The experience of leading scientific centers has shown that accurate medium-range forecasting of water and ice conditions in the Arctic requires coupled models of ocean and sea ice dynamics and thermodynamics. Thus, a data assimilation method that allows the generation of dynamically consistent ocean model fields while accounting for the state of sea ice can contribute to improving the accuracy of climate research and weather forecasts [5]. The importance of choosing a method for assimilating observational data for the Arctic region is also noted in [6].

This work is aimed at developing a coupled ocean and sea ice model with strongly coupled assimilation of available observational data and at implementing it for the Arctic region.

## 2. Coupled ocean and sea ice model with observational data assimilation

**2.1. Coupled ocean-ice model.** In this work, we use a global coupled ocean and sea ice model consisting of the general circulation ocean model developed at the Institute of Numerical Mathematics and the Institute of Oceanology (INMIO model) [7] and the CICE 5.1 ice dynamics and thermodynamics model <sup>1</sup>, running on massively parallel

---

<sup>1</sup> Hunke, E.C., 2015. *CICE: The Los Alamos Sea Ice Model Documentation and Software User's Manual Version 5.1*. Technical report LA-CC-06-012. Los Alamos: Los Alamos National Laboratory, 116 p.

computers under the control of the Compact Modeling Framework (CMF) [8]. Validation of the coupled INMIO-CICE model was carried out in [9].

The ocean and sea ice models use a threepolar grid [10] with a nominal resolution of  $0.25^\circ$ . The number of ocean grid levels along the  $z$ -coordinate is 49, and the vertical step increases from 6 m at the surface to 250 m at the bottom in the deep-ocean part. Bottom topography data were interpolated from the ETOPO5 array <sup>2</sup>, excluding inland water bodies and small islands.

In this work, we use the same configuration of the coupled INMIO-CICE model with a resolution of  $0.25^\circ$  as that used in [11]. In particular, for the ocean, lateral momentum exchange is modeled by a biharmonic operator. The coefficient for this operator is scaled proportionally to the grid-cell area to the power of  $3/2$ , based on the assumption of a balance between parameterized lateral exchange and explicitly resolved advective transport [12]. The equatorial value of the coefficient is taken to be  $-1.5 \cdot 10^{11} \text{ m}^4/\text{s}$  in accordance with [13]. An additional biharmonic Smagorinsky term in the form presented in [12] is added to ensure numerical stability. Lateral mixing of heat and salt is approximated by a Laplacian operator. The value of the coefficient for this operator is  $300 \text{ m}^2/\text{s}$  at the equator and is scaled proportionally to the grid-cell area to the power of  $1/2$  [13]. Momentum advection is approximated by a central-difference scheme, while the flux-corrected transport scheme [14] is used for the advection of heat and salt. The fluxes of heat, mass, and momentum between the atmosphere and the ocean are calculated using bulk formulas from [15] for the atmospheric boundary layer.

In the CICE 5.1 model configuration, ice in each grid cell is divided into five thickness categories with one additional category for snow. Thus, the ice concentration array (i.e., the proportion of the grid-cell area covered by ice) for each category is used as the main variable characterizing the state of the ice in the model. The elastic-viscous-plastic approximation is used to model sea-ice rheology, and ice transport is performed using an upwind difference scheme. To describe temperature changes, a zero-layer thermodynamic model is used, in which ice is considered fresh and has zero heat capacity. A similar configuration of the CICE model is used in many key operational ocean forecasting centers, in particular in the TOPAZ system (Norway), consisting of a coupled ocean and sea-ice model (HYCOM-CICE) with data assimilation using the EnKF (ensemble Kalman filter) method [16].

The time step for the INMIO and CICE components is 10 minutes. The interaction between the ocean and ice models occurs every 20 minutes, with the ocean model transmitting to the ice model the temperature and salinity at the ocean surface, horizontal velocity components, the surface slope, the potential heat of freezing or melting of the upper computational cell, and the ice model transmitting, respectively, ice concentration, horizontal friction stress components, and freshwater, salt, heat, and penetrating shortwave-radiation fluxes.

Prior to the data assimilation experiments, a spin-up of the coupled model was carried out for the period from 01 January 2009 to 31 August 2019, during which

---

<sup>2</sup> National Geophysical Data Center, NESDIS, NOAA, U.S. Department of Commerce, 1986. *ETOPO5: Global Earth Topography, 5-Minute, from NGDC: Dataset.* <https://doi.org/10.5065/D62F7KG0>

the surface atmospheric fields were determined from the ERA-Interim reanalysis [17], and the model solution was saved every 10 days. These states, starting from 2011, were then used as ensemble elements to approximate the covariance matrices during the data assimilation experiments (see Section 2.3 and Table 1).

Within the framework of this work, the main attention is paid to assimilation issues; otherwise, we followed a compromise between simplicity, computational cost, and physical adequacy.

**2.2. Data assimilation based on the EnOI method.** The main equations of the EnOI method are as follows [18]:

$$\begin{aligned}x_a &= x_b + K(y_{\text{obs}} - Hx_b), \\ K &= BH^T(HBH^T + R)^{-1}.\end{aligned}$$

Here  $x_b$  (forecast) and  $x_a$  (analysis) are the vectors of the model solution before and after assimilation, of size  $n$ ;  $n$  is the product of the number of grid points and the number of unknowns;

$$\begin{aligned}n &= [2(\text{temperature and salinity}) \cdot 49 (\text{model levels}) + \\ &+ 2 (\text{ocean level and ice concentration})] \cdot 1440 \cdot 720 \approx 10^8;\end{aligned}$$

$y_{\text{obs}}$  is the observation vector of size  $m$ ;  $m$  is the number of observation points;  $K(n \times m)$  is the Kalman gain matrix;  $R(m \times m)$  is the covariance matrix of instrumental observation errors;  $H(m \times n)$  is the matrix projecting model values into observation space;  $B(n \times n)$  is the model error covariance matrix.

The main idea of the ensemble method is that the covariance matrix  $B$  is obtained from an ensemble of model state vectors (a sample) [19].

Let  $A_b = [x_b^1 \dots x_b^N] - [\bar{x}_b \dots \bar{x}_b]$  be the matrix of  $n \times N$  size, where  $N$  is the number of ensemble elements (usually no more than 100), whose columns are equal to the model state vectors minus the ensemble mean. That is:  $\bar{x}_b = \frac{1}{N}[x_b^1 + \dots + x_b^N]$ .

Then the model error covariance matrix constructed on the basis of this sample is:  $B^{\text{en}} = \frac{1}{N-1}A_b(A_b)^T$ .

**2.3. Software implementation of EnOI.** The data assimilation procedure is encapsulated in the Data Assimilation Service (DAS) of the CMF 3.0 platform [20]. The service runs in parallel on separate processor cores and can be used simultaneously for several model components (ocean, ice, atmosphere, etc.). There is no explicit dependence on model equations, difference schemes, or model parameterizations. Only the output data of model calculations in the form of ensemble vectors are used, on the basis of which the model error covariance matrix  $B$  is approximated.

The data transfer scheme between the ocean model (OCN), the sea-ice model (ICE), the services for boundary-condition exchange (coupler, CPL), data assimilation (DAS), and input-output of data (IOD) within the coupled model under the control of the CMF is shown in Fig. 1. Issues of parallel scaling of the INMIO-CMF system were discussed in [8].

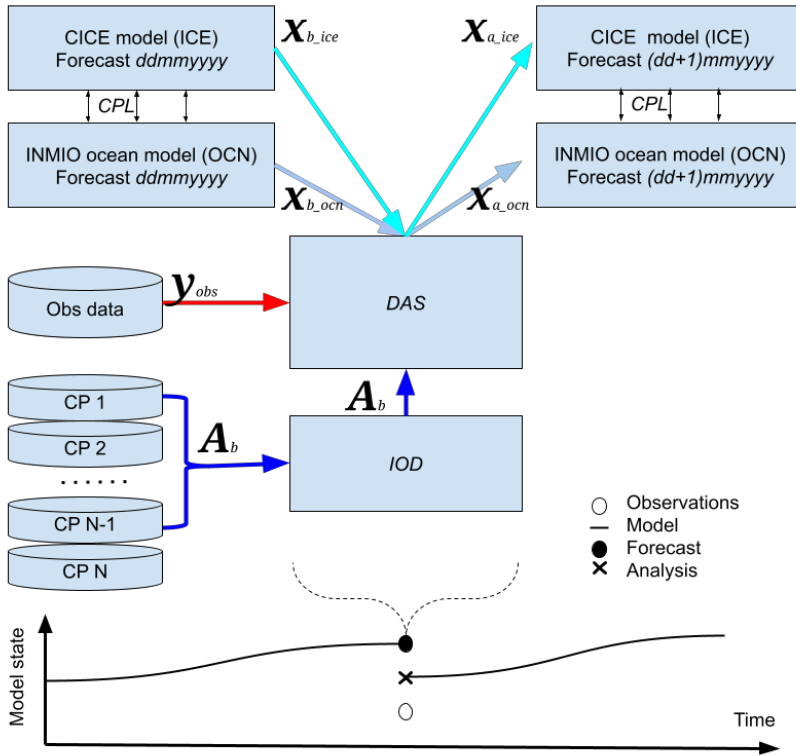


**Fig. 1.** Schematic diagram of data transfer between the ocean (OCN) and sea ice (ICE) models, the coupler (CPL), the Data Assimilation Service (DAS), and the service of file system operation (IOD) within the framework of CMF 3.0. Below is a timeline of changes in the model state vector during model integration and data assimilation

Once per model day, the state vectors of the ocean model  $x_b$  and the ice model  $x_b$  are transmitted via the cluster interconnect to the DAS service. In the DAS service, based on oceanic and ice observational data and using an ensemble of states for previous model years (which is asynchronously read from the file system once per model month), data assimilation is performed in a strongly coupled mode, after which the analysis vectors  $x_a$  of the ocean model and  $x_a$  of the ice model are sent back to the corresponding models and used as initial conditions for the next day of integration of the coupled model. The EnOI method requires integrating only one model, rather than  $N$  models, as in the EnKF method, because previously saved model fields (model checkpoints) for previous years of the simulation are used as the ensemble [21, 22].

When calling the DAS service to approximate the model-error covariance matrix  $B^{en}$ , we use an ensemble of ocean and sea-ice model states for the same or adjacent calendar month, but for previous years of the coupled INMIO-CICE model calculation. Specifically, each ensemble element includes three-dimensional arrays of temperature  $T(x, y, z)$  and salinity  $S(x, y, z)$ , as well as two-dimensional arrays of sea surface level  $SSL(x, y)$  and sea-ice concentration  $AICE(x, y)$ , combined into a one-dimensional array, with all physical data “nondimensionalized” by dividing by

the value of the characteristic error for each data type. The columns of the matrix  $A_b$  represent these vectors minus their ensemble mean (see Section 2.2).

The ensemble size was chosen to be 50 based on the rate of error reduction estimated in numerical experiments [23]. The model-error covariance matrix  $B^{\text{en}}$  calculated in this way takes into account the correlation between various model variables: sea level, ice concentration, temperature, and salinity at different model levels (Table 1). Thus, assimilation of even one type of observational data will correct the entire model state vector.

Table 1

**Composition and size of vectors  $x_a$ ,  $x_b$ ,  $y_{\text{obs}}$ , and matrix  $A_b$**

Parameter	Vectors of model state (forecast and analysis) $x_a, x_b$	Vector of observational data $y_{\text{obs}}$	Ensemble matrix $A_b$
Size	$n \approx 10^8$	$m \approx 10^5$	$N \times N^{**}$ ; $N = 50$
Composition	<u>Fields of INMIO model:</u> – water temperature $T^{3d}$ and salinity $S^{3d}$ (49 horizons); – ocean level $SSL^{2d}$ . <u>Fields of CICE ice model:</u> – ice concentration $AICE^{2d}$	Observational data: – Argo profiles ( $T, S$ ), $\times 10^3$ (profiles per day); – ADT level of along-track, Jason-3, AVISO project, $\times 10^3$ (points per day); – sea ice concentration SIC, EUMETSAT OSI SAF project, [0,1; 0,9] *	CP models for 2011–2019 are selected starting from the DDMM analysis date $\pm 1$ month

\* To derive information on the ice-edge boundary, the points where the concentration is within these limits are selected during preprocessing.

\*\* Amount of ensemble elements.

The following observational data are used:

- *in situ* temperature and salinity profiles obtained from Argo floats <sup>3</sup>;
- satellite altimetry data on absolute dynamic topography (ADT) from the AVISO project (Jason-3 satellite observations) <sup>4</sup>;
- AMSR-2 sea-ice concentration data obtained using the EUMETSAT Ocean and Sea Ice Satellite Application Facility (OSI SAF) satellite system <sup>5</sup>.

#### 2.4. Features of data assimilation in the coupled ocean-ice model.

The widely used weakly coupled data assimilation in the form of “nudging” for the CICE 5.1 model and the EnOI method for the INMIO model proved unsuitable for our tasks. Numerical experiments revealed that during calculations with

<sup>3</sup> SEANOE, 2023. Argo Float Data and Metadata from Global Data Assembly Centre (Argo GDAC): Dataset. <https://doi.org/10.17882/42182>

<sup>4</sup> Bannoura, W., Parisot, F., Vaze, P. and Zaouche, G., 2013. *Jason-3 Project Status: Presentation*. Boulder, 26 slides. [online] Available at: [http://www.avisio.altimetry.fr/fileadmin/documents/OSTST/2013/oral/Zaouche\\_Jason-3\\_mission\\_status\\_v1.pdf](http://www.avisio.altimetry.fr/fileadmin/documents/OSTST/2013/oral/Zaouche_Jason-3_mission_status_v1.pdf) [Accessed: 10 February 2026].

<sup>5</sup> Tonboe, R., Lavelle, J., Pfeiffer, R.-H. and Howe, E., 2017. *Product User Manual for OSI SAF Global Sea Ice Concentration. Product OSI-401-b. Version 1.6: Technical report*. OSI SAF, 25 p. [online] Available at: [https://osisaf-hl.met.no/sites/osisaf-hl/files/user\\_manuals/osisaf\\_cdop3\\_ss2\\_pum\\_ice-conc\\_v1p6.pdf](https://osisaf-hl.met.no/sites/osisaf-hl/files/user_manuals/osisaf_cdop3_ss2_pum_ice-conc_v1p6.pdf) [Accessed: 10 February 2026].

the INMIO-CICE model using data assimilation according to this scheme, inconsistencies between the ocean and ice model fields regularly occurred. As a consequence, this led to a computational failure due to violations of the dynamic-thermodynamic balance and to physically incorrect model fields.

This indicates the presence of a complex dynamic-thermodynamic balance in the CICE 5.1 model, where a sharp change in one of the ice-model fields or the receipt of inconsistent boundary conditions from the ocean model can lead to errors in the calculation of other fields. Thus, it is necessary to coordinate the thermodynamic and dynamic fields at the stage of their correction using data assimilation, in particular, to coordinate the temperature and salinity fields in the ocean, as well as the concentration and thickness fields in the ice model.

As a result, a *strongly coupled data assimilation* approach was implemented in the coupled ocean-ice model, in which assimilation for both components is performed in a separate DAS service with a combined analysis of the calculated fields from the two models. However, for smooth mutual adaptation, it was necessary to implement an interface for the ice model. The main goal of this interface is to change the internal variables of the CICE 5.1 model so that the total ice concentration in a grid cell corresponds to that transmitted to the procedure from the DAS assimilation service.

The change in model variables occurs in two stages. At the first stage, cells in which the model solution has a nonzero concentration are identified, and this concentration is at least  $\alpha_{\text{limit}}$  (experimentally chosen as 0.01) of the target concentration obtained from the DAS block. A model-solution correction procedure is performed for these cells; during this procedure, some of the properties listed below are preserved. For other cells in which, according to the DAS service, ice should appear, the ice field is reinitialized. The implementation features of these two steps are described below.

One of the main difficulties is the need to correct ice fields by an integral characteristic (concentration), while in the ice model the prognostic variables are the partial concentrations for each thickness category. In order to preserve information about the structure of the model solution, changes in the partial concentration and partial volume of ice and snow occur proportionally to the distribution of concentration among the categories of the original model state. This corresponds to a proportional increase in the ice-thickness distribution function. In this case, the average ice thickness in each category and the total average ice thickness remain unchanged, and ice does not transit between categories.

The internal dynamic and thermodynamic variables of the ice model are not corrected during this procedure. From the point of view of ice thermodynamics, such a procedure does not lead to an imbalance, since the basic equations for each category are one-dimensional and are written for an ice column whose thickness does not change. The influence of this procedure on the dynamic submodel will be studied in future work, but in practice no significant noise generation in the dynamic variables of the solution was observed.

When reinitializing the model solution (for example, when it is necessary to form ice in the model over open water), the procedure, in addition to changing the arrays of concentration and ice volume in the CICE model, must also determine other variables in this cell. This procedure largely follows the implementation of model-field initialization in the original model. It is assumed that, in the absence of information on the thickness of the observed ice field (as in this experiment), the procedure sets the ice distribution among thickness categories in accordance with a quadratic function whose maximum corresponds to a preselected thickness  $h_{\text{new\_ice}}$  (experimentally chosen as 0.5 m). Additionally, the snow thickness (experimentally chosen as 0.1 m), surface temperature (the minimum of the atmospheric temperature and the freezing temperature), zero salinity and enthalpy of fresh ice are set. The dynamic variables are set to zero.

Thus, a gradual change in ice concentration occurs. The advantage over weakly coupled assimilation is that during the subsequent correction of ice concentration, other model fields (water temperature, salinity, and sea level) are also taken into account, which ensures their consistency not only through the boundary-condition exchange mechanism.

### 3. Results and discussion

#### Experiments on modeling the circulation of water and sea ice in the Arctic in 2020

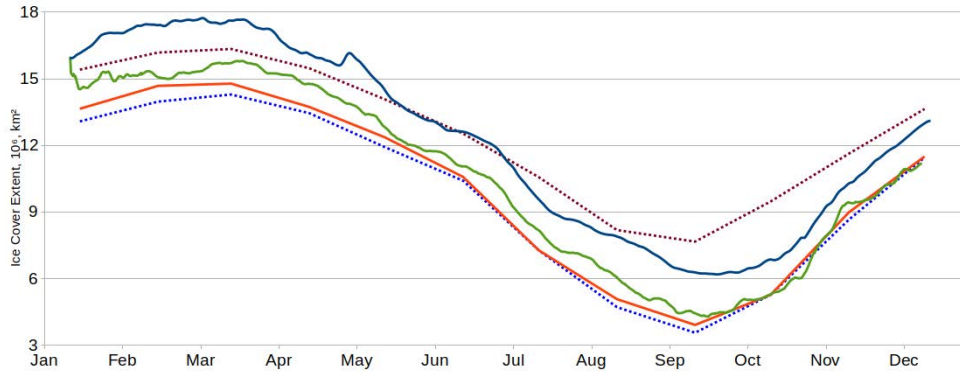
The proposed approach to data assimilation in a strongly coupled regime was tested in a series of numerical experiments with the global coupled ocean-ice model INMIO-CICE with a resolution of 0.25°. The model was forced with atmospheric data from operational forecasts (Global Forecast System, GFS) for the period from 01 January 2020 to 31 December 2020. Two experiments were performed:

- **h01** – a control run without observational data assimilation;
- **h02** – an experiment with strongly coupled assimilation of water temperature, salinity, sea surface height, and sea-ice concentration data.

**3.1. Arctic ice extent in 2020.** Fig. 2 and Table 2 compare the annual changes in sea-ice extent in the Northern Hemisphere in 2020 obtained in experiments **h01** (without DAS) and **h02** (DAS) with the analysis data provided by the National Snow and Ice Data Center (NSIDC) <sup>6</sup>. It can be seen that due to observational data assimilation it was possible to significantly improve the accuracy of sea-ice cover modeling. The average annual error decreased from 27% to 7%. Fig. 2 also shows that in the experiment **h01**, without data assimilation, the obtained ice area did not even fit into the “corridor” of interannual variability for 1979–2019. At the same time, with data assimilation in experiment **h02**, a clear correspondence between the model results and the analysis data can be seen.

---

<sup>6</sup> NCEI, 2021. *Sea Ice and Snow Cover Extent*. [online] Available at: <https://www.ncdc.noaa.gov/snow-and-ice/extent/> [Accessed: 10 February 2026].



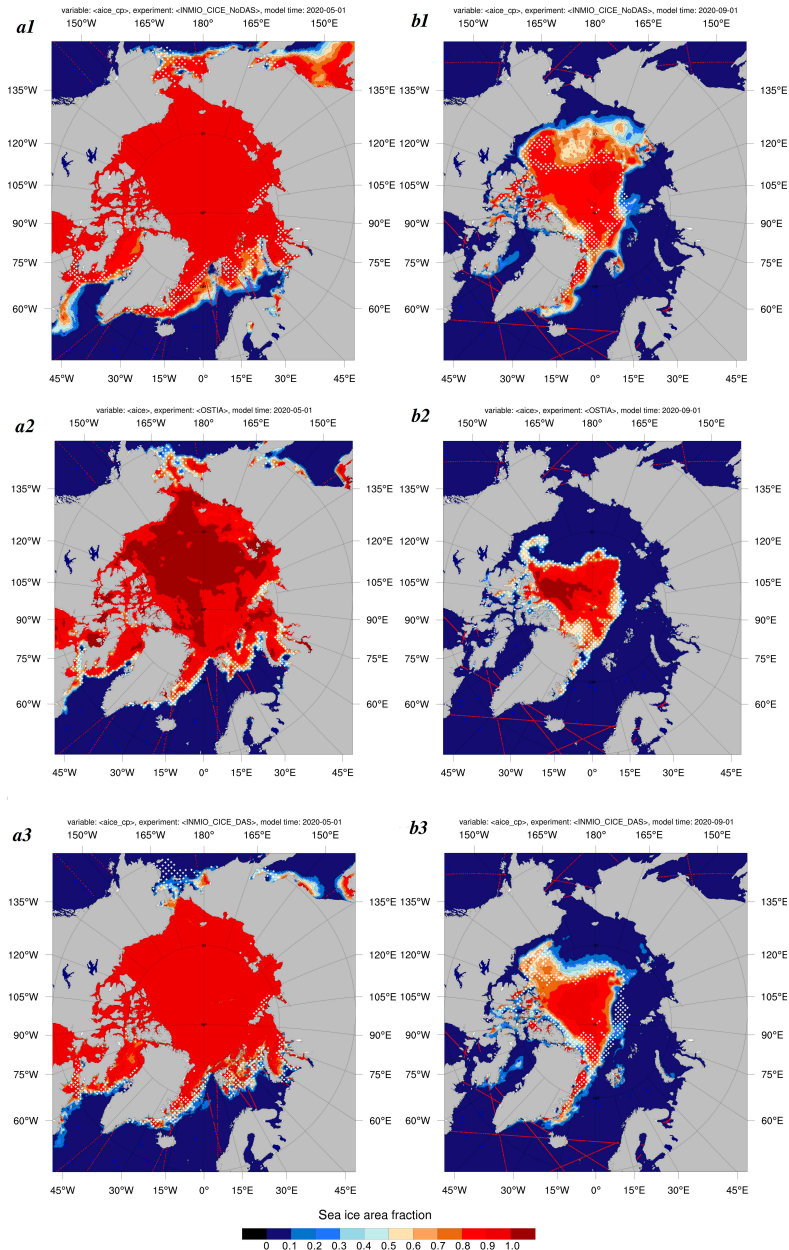
**Fig. 2.** Sea-ice extent in the Northern Hemisphere for 2020 based on NSIDC data and the INMIO-CICE modeling results: control experiment *h01* without data assimilation (blue solid line) and experiment *h02* with data assimilation via the DAS service (green solid line). The blue and brown dotted lines show the minimum and the maximum of sea-ice extent, respectively, based on NSIDC data for 1979–2019

Table 2

**Comparison of monthly sea-ice extent in the Northern Hemisphere for 2020 based on NSIDC data and the INMIO-CICE modeling results without (control experiment *h01*) and with (experiment *h02*) data assimilation via the DAS service**

Month	<i>h01</i> · 10 <sup>6</sup> , km <sup>2</sup>	Deviation <i>h01</i> minus NSIDC, %	<i>h02</i> · 10 <sup>6</sup> , km <sup>2</sup>	Deviation <i>h02</i> minus NSIDC, %	NSIDC · 10 <sup>6</sup> , km <sup>2</sup>
January	16.63	22	14.97	10	13.65
February	17.45	19	15.17	3	14.68
March	17.50	18	15.58	5	14.78
April	16.13	17	14.66	7	13.73
May	14.44	17	12.73	3	12.36
June	12.49	18	11.02	4	10.58
July	9.62	32	8.09	11	7.28
August	7.77	53	5.93	17	5.08
September	6.42	64	4.56	16	3.92
October	7.03	33	5.55	5	5.28
November	10.28	14	9.05	1	8.99
December	13.32	13	11.86	1	11.77
<b>Average for 2020</b>	<b>12.42</b>	<b>27</b>	<b>10.76</b>	<b>7</b>	<b>10.18</b>

**3.2. Analysis of forecast accuracy in the Arctic.** Fig. 3 shows ice-concentration fields obtained in experiments *h01* and *h02* in comparison with independent OSTIA (Operational Sea Surface Temperature and Sea Ice Analysis) observational data [24] for 1 May and 1 September (the months when active ice melting in the Arctic begins and ends).



**Fig. 3.** Ice-concentration fields for 1 May (*a1*, *a2*, *a3*) and 1 September (*b1*, *b2*, *b3*), 2020: *a1* and *b1* correspond to the control experiment *h01*; *a3* and *b3* correspond to experiment *h02* with DAS assimilation (white crosses indicate ice-cover boundary according to the OSI SAF data and concentration in the range 0.1...0.9; blue triangles denote Argo floats; red crosses show satellite altimetry data along the Jason-3 satellite track); *a2* and *b2* are based on independent OSTIA observational data

It can be seen from the figures that the model fields without assimilation are too smooth, and the eddy structures characteristic of models with  $0.25^\circ$  resolution are not reproduced. It is also worth noting that the coupled model overestimates the amount of ice, and the ice-cover boundary is reproduced incorrectly. Due to assimilation in experiment *h02*, the ice-cover area significantly decreased, so that the model solution became more consistent with the OSTIA data.

Figs. 4 and 5 show graphs of the standard errors (RMS errors) of the water-temperature fields in comparison with Argo float data and of ice concentration at points in the vicinity of the ice edge, where concentration is within the range  $[0.1; 0.9]$ , north of  $30^\circ\text{N}$ , for the control experiment without assimilation *h01* and for experiment *h02* before assimilation (forecast error) and after it (analysis error). The graphs show that assimilation provides the correct sign of the correction, and the difference between the errors in the forecast and in the control experiment is about  $0.5^\circ\text{C}$ . The average forecast error over the experiment is approximately  $1^\circ\text{C}$  for SST data and  $0.2$  for ice concentration. This is consistent with data from the Copernicus Marine Environment Monitoring Service (CMEMS) <sup>5</sup>, in which the RMS for the daily SST forecast is  $0.8^\circ\text{C}$ , and for ice concentration – about  $0.2$ . The methodology applied to calculate errors for sea-ice concentration is presented in [25].

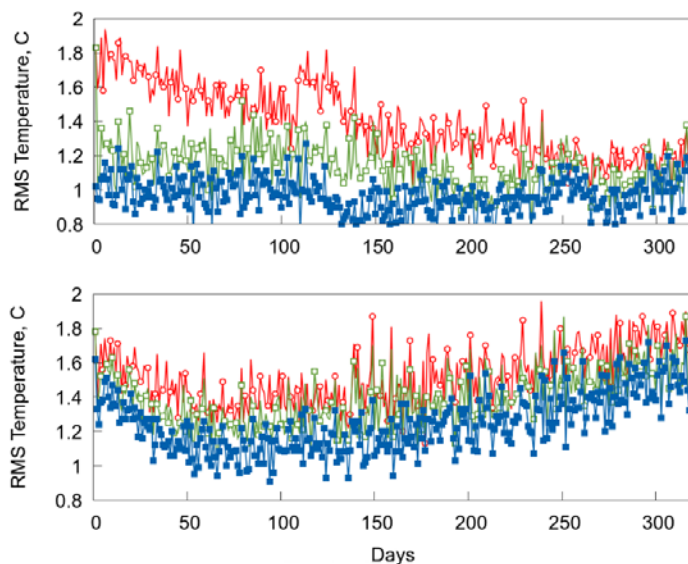


**Fig. 4.** Standard error of water temperature for the control experiment without assimilation, *h01* (red line), and errors in the forecast (green line) and analysis (blue line) in the experiment *h02* with assimilation, for the temperature field at depths of 3 m (*top*) and 105 m (*bottom*) compared with the Argo data

Observational data assimilation using standard methods in a model of a dynamically complex nonlinear system of the two-phase ice-ocean medium is associated with difficulties: data come from various platforms with different spatiotemporal characteristics and often characterize only one parameter of the system, which leads to imbalance and, as a consequence, to nonphysical anomalies in the model solution, which in turn may lead to forecast instability.

The strongly coupled data assimilation approach proposed in this work for coupled ice-ocean models, borrowed from meteorological forecasting systems [4, 26], allows all variables and components to be processed simultaneously in a single analysis, which reduces the risk of imbalance.

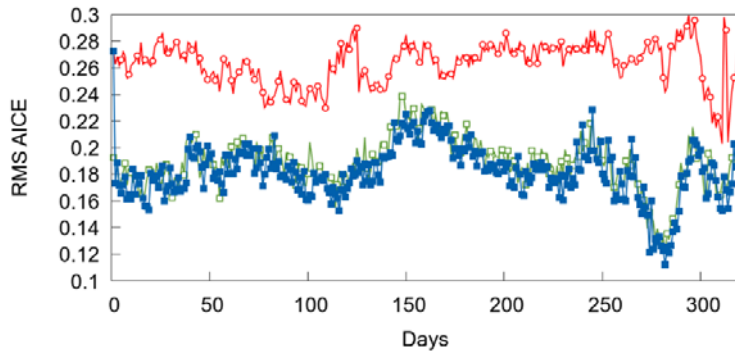


**Fig. 5.** Standard error of ice concentration for the control experiment without assimilation, **h01** (red line), and the errors of forecast (green line) and analysis (blue line) in experiment **h02** with assimilation, for the ice-concentration field compared with the OSI SAF data

The retrospective simulation performed for 2020 revealed that the developed method provides accuracy comparable to that of other modern operational sea-ice forecasting systems [27]. The positive effect of assimilation is maintained at all considered horizons and throughout the experiment, which confirms the effectiveness of the strongly coupled approach for Arctic forecasting tasks.

### Conclusion

In this work, a strongly coupled approach to data assimilation in an ice-ocean model is proposed, implemented, and tested for the Arctic region for the first time in Russia. The approach is based on the simultaneous analysis of a wide range of assimilated observational data (water temperature and salinity from Argo, absolute dynamic topography from AVISO, and sea-ice concentration OSI SAF). The strongly coupled method is implemented within a forecast model based on the parallel computing software system INMIO-CICE5.1-CMF3.1-DAS.

Numerical experiments for 2020 revealed that strongly coupled data assimilation allows:

- reducing the average annual error in reproducing ice extent from 27% to 7% relative to the NSIDC data;
- reducing the water-temperature RMS error to 1.0 °C, and the RMS error of ice concentration in the marginal ice zone to 0.2;
- improving the agreement of model fields with independent OSTIA data, especially during periods of active ice melting.

The method and its program code can be adapted and applied to other coupled ice-ocean models with data assimilation. The code will be made publicly available on the website <http://model.ocean.ru>. Further research will focus on increasing the spatiotemporal scale of the coupled ocean-sea-ice model and incorporating new observational data for assimilation.

## REFERENCES

1. Guemas, V., Blanchard-Wrigglesworth, E., Chevallier, M., Day, J.J., Déqué, M., Doblas-Reyes, F.J., Fučkar, N.S., Germe, A., Hawkins, E. [et al.], 2016. A Review on Arctic Sea-Ice Predictability and Prediction on Seasonal to Decadal Time-Scales. *Quarterly Journal of the Royal Meteorological Society*, 142(695), pp. 546-561. <https://doi.org/10.1002/qj.2401>
2. Skachko, S., Buehner, M., Laroche, S., Lalpalmé, E., Smith, G., Roy, F., Surcel-Colan, D., Bélanger, J.-M. and Garand, L., 2019. Weakly Coupled Atmosphere–Ocean Data Assimilation in the Canadian Global Prediction System (v1). *Geoscientific Model Development*, 12(12), pp. 5097-5112. <https://doi.org/10.5194/gmd-12-5097-2019>
3. Brassington, G.B., Martin, M.J., Tolman, H.I., Akella, S., Balmeseda, M., Chambers, C.R.S., Chassignet, E., Cummings, J.A., Drillet, Y. [et al.], 2015. Progress and Challenges in Short- to Medium-Range Coupled Prediction. *Journal of Operational Oceanography*, 8(S2), pp. s239-s258. <https://doi.org/10.1080/1755876X.2015.1049875>
4. Penny, S.G. and Hamill, T.M., 2017. Coupled Data Assimilation for Integrated Earth System Analysis and Prediction. *Bulletin of the American Meteorological Society*, 98(7), pp. ES169-ES172. <https://doi.org/10.1175/BAMS-D-17-0036.1>
5. Kimmritz, M., Counillon, F., Bitz, C.M., Massonnet, F., Bethke, I. and Gao, Y., 2018. Optimising Assimilation of Sea Ice Concentration in an Earth System Model with a Multicategory Sea Ice Model. *Tellus A: Dynamic Meteorology and Oceanography*, 70(1), 1435945. <https://doi.org/10.1080/16000870.2018.1435945>
6. Fomin, V.V. and Diansky, N.A., 2023. Methods of Assimilation of Sea Surface Temperature Satellite Data and Their Influence on the Reconstruction of Hydrophysical Fields of the Black, Azov, and Marmara Seas Using the Institute of Numerical Mathematics Ocean Model (INMOM). *Russian Meteorology and Hydrology*, 48(2), pp. 97-108. <https://doi.org/10.3103/S1068373923020024>
7. Ibrayev, R.A., Khabeev, R.N. and Ushakov, K.V., 2012. Eddy-Resolving 1/10° Model of the World Ocean. *Izvestiya, Atmospheric and Oceanic Physics*, 48(1), pp. 37-46. <https://doi.org/10.1134/S0001433812010045>
8. Kalmykov, V.V., Ibrayev, R.A., Kaurkin, M.N. and Ushakov, K.V., 2018. Compact Modeling Framework v3.0 for High-Resolution Global Ocean–Ice–Atmosphere Models. *Geoscientific Model Development*, 11(10), pp. 3983-3997. <https://doi.org/10.5194/gmd-11-3983-2018>
9. Kalnitskii, L.Y., Kaurkin, M.N., Ushakov, K.V. and Ibrayev, R.A., 2020. Seasonal Variability of Water and Sea-Ice Circulation in the Arctic Ocean in a High-Resolution Model. *Izvestiya, Atmospheric and Oceanic Physics*, 56(5), pp. 522-533. <https://doi.org/10.1134/S0001433820050060>
10. Murray, R.J., 1996. Explicit Generation of Orthogonal Grids for Ocean Models. *Journal of Computational Physics*, 126(2), pp. 251-273. <https://doi.org/10.1006/jcph.1996.0136>
11. Fadeev, R., Ushakov, K., Tolstykh, M., Ibrayev, R., Shashkin, V. and Goyman, G., 2019. Supercomputing the Seasonal Weather Prediction. In: V. Voevodin and S. Sobolev, eds., 2019. *Supercomputing*. Cham: Springer, pp. 415-426. [https://doi.org/10.1007/978-3-030-36592-9\\_34](https://doi.org/10.1007/978-3-030-36592-9_34)
12. Griffies, S.M. and Hallberg, R.W., 2000. Biharmonic Friction with a Smagorinsky-Like Viscosity for Use in Large-Scale Eddy-Permitting Ocean Models. *Monthly Weather Review*, 128(8), pp. 2935-2946. [https://doi.org/10.1175/1520-0493\(2000\)128<2935:BFWASL>2.0.CO;2](https://doi.org/10.1175/1520-0493(2000)128<2935:BFWASL>2.0.CO;2)
13. Dussin, R., Treguier, A.M., Molines, J.M., Barnier, B., Penduff, T., Brodeau, L. and Madec, G., 2009. *Definition of the Interannual Experiment ORCA025-B83, 1958-2007*. LPO Report 09-02. Brest, France: Laboratoire de Physique des Océans, 37 p.
14. Zalesak, S.T., 1979. Fully Multidimensional Flux-Corrected Transport Algorithms for Fluids. *Journal of Computational Physics*, 31(3), pp. 335-362. [https://doi.org/10.1016/0021-9991\(79\)90051-2](https://doi.org/10.1016/0021-9991(79)90051-2)
15. Launiainen, J. and Vihma, T., 1990. Derivation of Turbulent Surface Fluxes – An Iterative Flux-Profile Method Allowing Arbitrary Observing Heights. *Environmental Software*, 5(3), pp. 113-124. [https://doi.org/10.1016/0266-9838\(90\)90021-W](https://doi.org/10.1016/0266-9838(90)90021-W)
16. Sakov, P., Counillon, F., Bertino, L., Lisæter, K.A., Oke, P.R. and Korabely, A., 2012. TOPAZ4: An Ocean-Sea Ice Data Assimilation System for the North Atlantic and Arctic. *Ocean Science*, 8(4), pp. 633-656. <https://doi.org/10.5194/os-8-633-2012>
17. Dee, D.P., Uppala, S.M., Simmons, A.J., Berrisford, P., Poli, P., Kobayashi, S., Andrae, U., Balmeseda, M.A., Balsamo, G. [et al.], 2011. The ERA-Interim Reanalysis: Configuration and Performance of the Data Assimilation System. *Quarterly Journal of the Royal Meteorological Society*, 137(656), pp. 553-597. <https://doi.org/10.1002/qj.828>
18. Evensen, G., 2006. *Data Assimilation: The Ensemble Kalman Filter*. Berlin; Heidelberg: Springer-Verlag, 307 p. <https://doi.org/10.1007/978-3-642-03711-5>

19. Evensen, G., 2003. The Ensemble Kalman Filter: Theoretical Formulation and Practical Implementation. *Ocean Dynamics*, 53(4), pp. 343-367. <https://doi.org/10.1007/s10236-003-0036-9>
20. Kaurkin, M., Ibrayev, R. and Koromyslov, A., 2016. EnOI-Based Data Assimilation Technology for Satellite Observations and ARGO Float Measurements in a High Resolution Global Ocean Model Using the CMF Platform. In: V. Voevodin and S. Sobolev, eds., 2016. *Supercomputing*. Cham: Springer, pp. 57-66. [https://doi.org/10.1007/978-3-319-55669-7\\_5](https://doi.org/10.1007/978-3-319-55669-7_5)
21. Sakov, P. and Sandery, P.A., 2015. Comparison of EnOI and EnKF Regional Ocean Reanalysis Systems. *Ocean Modelling*, 89, pp. 45-60. <https://doi.org/10.1016/j.ocemod.2015.02.003>
22. Oke, P.R., Brassington, G.B., Griffin, D.A. and Schiller, A., 2010. Ocean Data Assimilation: A Case for Ensemble Optimal Interpolation. *Australian Meteorological and Oceanographic Journal*, 59, pp. 67-76.
23. Kaurkin, M.N., Ibrayev, R.A. and Belyaev, K.P., 2016. ARGO Data Assimilation into the Ocean Dynamics Model with High Spatial Resolution Using Ensemble Optimal Interpolation (EnOI). *Oceanology*, 56(6), pp. 774-781. <https://doi.org/10.1134/S0001437016060059>
24. Good, S., Fiedler, E., Mao, C., Martin, M.J., Maycock, A., Reid, R., Roberts-Jones, J., Searle, T., Waters, J. [et al.], 2020. The Current Configuration of the OSTIA System for Operational Production of Foundation Sea Surface Temperature and Ice Concentration Analyses. *Remote Sensing*, 12(4), 720. <https://doi.org/10.3390/rs12040720>
25. Melsom, A., Palerme, C. and Müller, M., 2019. Validation Metrics for Ice Edge Position Forecasts. *Ocean Science*, 15(3), pp. 615-630. <https://doi.org/10.5194/os-15-615-2019>
26. Fanjul, E.A., Ciliberti, S.A., Bahurel, P., Aouf, L., Bertino, L., Coppini, G., Diaz-Hernandez, G., Davidson, F., Gutknecht, E. [et al.], 2022. *Implementing Operational Ocean Monitoring and Forecasting Systems*. Paris, France: IOC-UNESCO, 376 p. <https://doi.org/10.48670/ETOOFS>
27. Kalnay, E., Sluka, T., Yoshida, T., Da, C. and Mote, S., 2023. Review Article: Towards Strongly Coupled Ensemble Data Assimilation with Additional Improvements from Machine Learning. *Nonlinear Processes in Geophysics*, 30(2), pp. 217-236. <https://doi.org/10.5194/npg-30-217-2023>

Submitted 23.10.2025; approved after review 29.10.2025;  
accepted for publication 28.01.2026.

*About the authors:*

**Maksim N. Kaurkin**, Researcher, Ocean and Sea Climate Variability Modeling Group, Shirshov Institute of Oceanology, Russian Academy of Sciences (36 Nakhimovsky Ave., Moscow, 117997, Russian Federation), CSc. (Phys.-Math.), **SPIN-code: 8374-6238**, **Scopus Author ID: 57190488613**, **ORCID ID: 0000-0002-0921-3630**, **ResearcherID: S-1416-2016**, [kaurkin.mn@ocean.ru](mailto:kaurkin.mn@ocean.ru)

**Leonid Yu. Kalnitskii**, Leading Engineer, Ocean and Sea Climate Variability Modeling Group, Shirshov Institute of Oceanology, Russian Academy of Sciences (36, Nakhimovsky Prospekt, Moscow, 117997, Russian Federation), **Scopus Author ID: 57219609143**, **ORCID ID: 0009-0005-4023-2257**, [leonid.kalnitsckij@yandex.ru](mailto:leonid.kalnitsckij@yandex.ru)

**Konstantin V. Ushakov**, Senior Research Associate, Ocean and Sea Climate Variability Modeling Group, Shirshov Institute of Oceanology, Russian Academy of Sciences (36 Nakhimovsky Ave., Moscow, 117997, Russian Federation), CSc. (Phys.-Math.), **SPIN-code: 6997-1295**, **Scopus Author ID: 55015342700**, **ORCID ID: 0000-0002-8454-9927**, **ResearcherID: U-6185-2017**, [ushakovkv@mail.ru](mailto:ushakovkv@mail.ru)

**Rashit A. Ibrayev**, Chief Researcher, Marchuk Institute of Numerical Mathematics, Russian Academy of Sciences (8 Gubkina Str., Moscow, 119333, Russian Federation); Shirshov Institute of Oceanology, Russian Academy of Sciences (36 Nakhimovsky Ave., Moscow, 117997, Russian Federation), DSc. (Phys.-Math.), Corresponding Member of RAS, **SPIN-code: 9003-9192**, **Scopus Author ID: 6602387822**, **ResearcherID: S-6750-2016**, **ORCID ID: 0000-0002-9099-4541**, [ibrayev@mail.ru](mailto:ibrayev@mail.ru)

*Contribution of the co-authors:*

**Maksim N. Kaurkin** – designed, implemented, and tested the Data Assimilation Service, carried out numerical experiments, and wrote the first draft of the manuscript

**Leonid Yu. Kalnitskii** – was responsible for operating the CICE sea ice model

**Konstantin V. Ushakov** – designed and developed the INMIO model and physical coupling algorithms

**Rashit A. Ibrayev** – designed and developed the INMIO model and physical coupling algorithms

*The authors have read and approved the final manuscript.*

*The authors declare that they have no conflict of interest.*